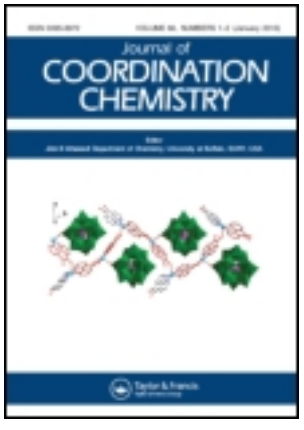

Journal of Coordination Chemistry
Publication details, including instructions for authors and subscription information:
http://www.tandfonline.com/loi/gcoo20

Synthesis and structural characterization of mono- and dinuclear Ni^{II} and Pd^{II} complexes derived from tetradentate 1,7-bis-(pyridin-2-yl)-2,6-diaza-1,6-heptadiene

J. Roberto Pioquinto-Mendoza [a], David G. Olvera-Mendoza [a], Noemí Andrade-López [a], José G. Alvarado-Rodríguez [a], Rafael Moreno-Esparza [b] & Marcos Flores-Álamo [b]

[a] Centro de Investigaciones Químicas, Universidad Autónoma del Estado de Hidalgo, Hgo, México

[b] Facultad de Química (UNAM), Ed. B. Ave. Universidad 3000, Coyoacán, México

Published online: 21 Jun 2013.

To cite this article: J. Roberto Pioquinto-Mendoza, David G. Olvera-Mendoza, Noemí Andrade-López, José G. Alvarado-Rodríguez, Rafael Moreno-Esparza & Marcos Flores-Álamo (2013) Synthesis and structural characterization of mono- and dinuclear Ni^{II} and Pd^{II} complexes derived from tetradentate 1,7-bis-(pyridin-2-yl)-2,6-diaza-1,6-heptadiene, Journal of Coordination Chemistry, 66:14, 2477-2488, DOI: 10.1080/00958972.2013.806985

To link to this article: http://dx.doi.org/10.1080/00958972.2013.806985

Journal of Coordination Chemistry, 2013
Vol. 66, No. 14, 2477–2488, http://dx.doi.org/10.1080/00958972.2013.806985

Synthesis and structural characterization of mono- and dinuclear Ni^{II} and Pd^{II} complexes derived from tetradentate 1,7-*bis*-(pyridin-2-yl)-2,6-diaza-1,6-heptadiene

J. ROBERTO PIOQUINTO-MENDOZA†, DAVID G. OLVERA-MENDOZA†
NOEMÍ ANDRADE-LÓPEZ*†, JOSÉ G. ALVARADO-RODRÍGUEZ†
RAFAEL MORENO-ESPARZA‡ and MARCOS FLORES-ÁLAMO‡

†Centro de Investigaciones Químicas, Universidad Autónoma del Estado de Hidalgo, Hgo, México
‡Facultad de Química (UNAM), Ed. B. Ave. Universidad 3000, Coyoacán, México

(*Received 7 December 2012; in final form 22 March 2013*)

The reaction of Schiff base 1,7-*bis*-(pyridin-2-yl)-2,6-diaza-1,6-heptadiene (**L**) with either $NiCl_2{\cdot}6H_2O$ or $[Pd^{II}Cl_2(CH_3CN)_2]$/$Na[BF_4]$ in 1 : 1 stoichiometry yielded mononuclear ionic complexes, *trans*-$[Ni^{II}(\mathbf{L})(H_2O)_2]Cl_2{\cdot}3H_2O$ (**1**·$3H_2O$) and $[Pd^{II}(\mathbf{L})][BF_4]_2$ (**2**), respectively; the reaction of **L** with $[Pd^{II}Cl_2(CH_3CN)_2]$ in 1 : 2 ratio yielded dinuclear *cis*-$[Pd^{II}{}_2(\mu\text{-}\mathbf{L})Cl_4]$ (**3**). Complexes **1–3** were characterized by vibrational spectroscopy and X-ray diffraction; diamagnetic **2** and **3** were also characterized by NMR in solution. The molecular structures of **1** and **2** displayed tetradentate coordination of **L** with formation of two five-membered and one six-membered chelate rings for both complexes. In **3**, **L** showed bidentate coordination mode for each pyridylimine toward Pd^{II}. Complex **1** has distorted octahedral geometry around Ni^{II} and an extended hydrogen-bond network; distorted square planar geometry around Pd^{II} in **2** and **3** was observed.

Keywords: Ni^{II} and Pd^{II} complexes; Schiff ligands; X-ray structures; Hydrogen-bond network

1. Introduction

A number of studies of compounds derived from pyridyl- and *bis*-(pyridyl)imine ligands have been carried out related with anticancer [1–4] and antimicrobial [3, 5] properties and for DNA-binding complexes [6–8]. In addition, several palladium complexes of pyridylimines have been used in Suzuki cross-coupling reactions [9], in norbornene [10] and acetylene [11] polymerization, in ethylene oligomerization [12], and in olefin cyclopropanation reactions [13]. Other palladium complexes of pyridylimines have been widely used in material sciences [14] because of their magnetic [14–17] and luminescent [18–20] properties. In environmental studies, pyridyl ligands have been utilized for trapping heavy metals such as Hg^{II} [18], Cd^{II} [18, 21], and Pb^{II} [21]. Some pyridylimines [22] and their Ag^{I}, Zn^{II}, and Cd^{II} [23] derivatives have been utilized in the design of new π–π molecular aggregates. For pyridylimines containing a spacer between two pyridyliminic fragments,

*Corresponding author. Email: nandrade@uaeh.edu.mx

mono and dinuclear metal complexes of several transition metals have been reported; in these studies the coordination versatility of the pyridylimine ligands was observed because they behaved as either bi or tetradentate [22–32].

Continuing with our studies of coordination chemistry of Schiff bases, herein we describe the synthesis and characterization of Ni^{II} and Pd^{II} mononuclear complexes, **1** and **2**, respectively, and the Pd^{II} dinuclear complex **3** containing the potentially tetradentate 1,7-*bis*-(pyridin-2-yl)-2,6-diaza-1,6-heptadiene (**L**), where **L** displayed a bi and tetradentate behavior toward Ni^{II} and Pd^{II}.

2. Experimental

2.1. *Materials and measurements*

Solvents were dried according to standard methods and distilled before use. $PdCl_2$, $NiCl_2{\cdot}6H_2O$, pyridine-2-carboxaldehyde, and 1,3-propanediamine were purchased from Aldrich and used as received. The diimine 2-$C_5H_4NCH{=}N(CH_2)_3N{=}CH$(2-$C_5H_4N$) (**L**) was prepared by a modified method previously described [32]. Melting points were recorded on a Mel-Temp II apparatus and are reported without correction. Elemental analyses were performed on a Perkin–Elmer Series II CHNS/O Analyzer 2400. Infrared spectra were recorded on a FT–IR 200 Perkin–Elmer spectrophotometer from 4000 to 400 cm^{-1} using KBr pellets. Raman spectra in the solid state were recorded from 4000 to 100 cm^{-1} on a Perkin–Elmer spectrum GX NIR FT–Raman spectrophotometer with 10–280 mW laser power and 4 cm^{-1} resolution. NMR spectra were recorded on a Varian NMRS 400 spectrometer; ^{1}H (399.78 MHz), $^{11}B\{^{1}H\}$ (128.27 MHz), $^{13}C\{^{1}H\}$ (100.53 MHz), and $^{19}F\{^{1}H\}$ (376.14 MHz) spectra were obtained in DMSO-d_6. Chemical shifts (ppm) of ^{1}H and $^{13}C\{^{1}H\}$ spectra are relative to $Si(CH_3)_4$ (table 1); the chemical shifts (ppm) of $^{11}B\{^{1}H\}$ and $^{19}F\{^{1}H\}$ spectra are relative to the frequency of $BF_3{\cdot}OEt_2$ and $CFCl_3$, respectively. NMR assignments of **L** and for **2** and **3** were performed by 2-D heteronuclear and mononuclear experiments (COZY and HMQC). Suitable single-crystals of **1** (green crystals after three weeks), **2** (pale yellow crystals after 10 days), and **3** (yellowish-orange crystals after one month) were obtained by slow evaporation of an acetonitrile, acetonitrile-chloroform (4 : 1 ratio), and DMSO saturated solution, respectively. The single-crystal X-ray structure determinations for **1–3** were collected at 141 K on an Oxford Diffraction Gemini CCD diffractometer with graphite-monochromated Mo-Kα radiation ($\lambda = 0.71073$ Å). Data were integrated, scaled, sorted, and averaged using the CrysAlis software package [33].

The structures were solved by direct methods using SHELXTL NT Version 5.1 and refined by full-matrix least squares against F^2 [34]. All nonhydrogen atoms were refined anisotropically. The positions of hydrogens of water were found in the difference map. The position of the remaining hydrogens was fixed with a common isotropic displacement parameter. Crystallographic data are given in table 2 and selected bond distances and angles are given in table 3.

2.2. *Synthesis of Ni^{II} and Pd^{II} complexes 1–3*

Complexes **1–3** were synthesized according to the following general method; the scheme is shown in scheme 1 along with the numbering scheme used for the organic moiety.

General method: A mixture of $NiCl_2{\cdot}6H_2O$ or $[PdCl_2(CH_3CN)_2]$ in hot acetonitrile was added to a solution of **L** in 10 mL of chloroform. For **1** and **2** the mixture was stirred and

Table 1. ^{1}H and $^{13}C\{^{1}H\}$ NMR data for **L**, **2** and **3** at room temperature in DMSO-d_6 (numbering scheme is shown in scheme 1).

Compound	^{1}H chemical shift (δ in ppm)	$^{13}C\{^{1}H\}$ chemical shift (δ in ppm)
L	8.63 (ddd, 2H, H5, ^{3}J = 4.88, ^{4}J = 1.71, ^{5}J = 1.0 Hz)	162.1 (C6)
	8.36 (t; 2H, H6, ^{4}J = 1.27 Hz)	154.1 (C1)
	7.97 (dd, 2H, H2, ^{3}J = 7.81, ^{4}J = 1.13 Hz)	149.4 (C5)
	7.85 (ddd, 2H, H3, ^{3}J = 7.81, ^{3}J = 7.81, ^{4}J = 1.71 Hz)	137.0 (C3)
	7.44 (ddd, 2H, H4, ^{3}J = 7.81, ^{3}J = 4.88, ^{3}J = 1.0 Hz)	125.1 (C4)
	3.71 (t, 4H, C**H$_2$**N, ^{3}J = 6.83, ^{4}J = 1.27 Hz)	120.4 (C2)
	2.01 (q, 2H, C**H$_2$**CH$_2$N, ^{3}J = 6.83 Hz)	58.1 (**C**H$_2$N)
		31.5 (**C**H$_2$CH$_2$N)
2	8.96 (t, 2H, H6, ^{4}J = 1.74 Hz)	173.3 (C6)
	8.94 (dd, 2H, H5, ^{3}J = 5.38, ^{4}J = 0.98 Hz)	154.7 (C1)
	8.54 (ddd, 2H, H3, ^{3}J = 7.82, ^{3}J = 7.82, ^{4}J = 0.98 Hz)	151.8 (C5)
	8.32 (dd, 2H, H2, ^{3}J = 7.82, ^{4}J = 1.47 Hz)	143.2 (C3)
	8.04 (ddd, 2H, H4, ^{3}J = 7.82, ^{3}J = 5.38, ^{4}J = 1.47 Hz)	129.6 (C4)
	3.88 (s, b; 4H, C**H$_2$**N)	129.5 (C2)
	2.20 (s, b; 2H, C**H$_2$**CH$_2$N)	54.8 (**C**H$_2$N)
		28.6 (**C**H$_2$CH$_2$N)
3	8.87 (t, 2H, H6, ^{4}J = 1.73 Hz)	171.2 (C6)
	8.85 (dd, 2H, H5, ^{3}J = 5.37, ^{4}J = 1.48 Hz)	154.5 (C1)
	8.38 (ddd, 2H, H3, ^{3}J = 7.83, ^{3}J = 7.83, ^{4}J = 1.48 Hz)	150.7 (C5)
	8.18 (dd, 2H, H2, ^{3}J = 7.83, ^{4}J = 1.48 Hz)	142.0 (C3)
	7.89 (ddd, 2H, H4, ^{3}J = 7.83, ^{3}J = 5.37, ^{4}J = 1.48 Hz)	129.1 (C4)
	3.73 (s, vb, 4H, C**H$_2$**N)	128.5 (C2)
	1.86 (s, vb; 2H,C**H$_2$**CH$_2$N)	54.4 (**C**H$_2$N)
		28.8 (**C**H$_2$CH$_2$N)

refluxed for 24 and 2.5 h, respectively. For **3**, the mixture was stirred at room temperature for 3 h. In every case the solid obtained was filtered from the mixture; a green solid for **1** and yellow solids for **2** and **3** were obtained.

2.2.1. Synthesis of *trans*-[Ni^{II}(L)(H$_2$O)$_2$]Cl$_2$·3H$_2$O (1). $NiCl_2 \cdot 6H_2O$ (0.38 g, 1.59 mmol), acetonitrile (15 mL), **L** (0.40 g, 1.59 mmol), chloroform (10 mL). Yield 93% (0.347 g). M.p.: 228 °C (dec). Anal. Calcd for $C_{15}H_{26}Cl_2N_4O_5Ni$ (**1**) (%): C, 38.17; H, 5.55; N, 11.87. Found (%): C, 38.39; H, 5.45; N, 11.74. IR data (KBr, cm^{-1}): 3050, 3009 ($CH_{aromatics}$); 2918 (CH_2); 2850 (CH_2N); 1640 (C=N); 1599 (C=N, C=C).

2.2.2. Synthesis of [Pd^{II}(L)][BF$_4$]$_2$ (2). $[Pd^{II}Cl_2(CH_3CN)_2]$ (0.1 g, 0.39 mmol), acetonitrile (35 mL), $Na[BF_4]$ (0.085 g, 0.80 mmol), **L** (0.098 g, 0.39 mmol), chloroform (10 mL). Yield 97% (0.199 g). M.p.: 170 °C (dec). Anal. Calcd for $C_{15}H_{16}N_4B_2F_8Pd$ (**2**) (%): C, 33.84; H, 3.03; N, 10.52. Found (%): C, 34.13; H, 3.02; N, 10.18%. IR data (KBr, cm^{-1}): 3052, 2955 ($CH_{aromatics}$); 2921 (CH_2); 2851 (CH_2–N); 1639 (C=N); 1602 (C=N, C=C). NMR $^{11}B\{^{1}H\}$: δ (ppm, DMSO-d_6 at 25 °C) = 3.43; $^{19}F\{^{1}H\}$: δ (ppm, DMSO-d_6 at 25 °C) = −148.2.

2.2.3. Synthesis of *cis*-[Pd$^{II}_2$(μ-L)Cl$_4$] (3). $[Pd^{II}Cl_2(CH_3CN)_2]$ (0.10 g, 0.39 mmol), acetonitrile (35 mL), **L** (0.049 g, 0.19 mmol), chloroform (10 mL). Yield 93% (0.107 g).

Table 2. Selected crystallographic data for **1**–**3**.

	1	**2**	**3**
Formula	$C_{15}H_{26}Cl_2N_4O_5Ni$	$C_{15}H_{16}N_4B_2F_8Pd$	$C_{15}H_{16}Cl_4N_4Pd_2$
Formula weight	472.01	532.34	606.97
Crystal size (mm)	$0.41 \times 0.26 \times 0.23$	$0.58 \times 0.31 \times 0.23$	$0.25 \times 0.08 \times 0.07$
Crystal system	Triclinic	Monoclinic	Orthorhombic
Space group	$P-1$	C_2/c	$P2_12_12_1$
a (Å)	9.3262(4)	14.1898(5)	10.2590(3)
b (Å)	10.0632(4)	10.0285(3	12.8066(3)
c (Å)	11.4789(5)	13.3513(5)	14.5304(4)
α (°)	85.301(3)	90	90
β (°)	88.715(4)	105.997(4)	90
γ (°)	75.128(4)	90	90
V (Å^3)	1037.72(8)	1826.35(11)	1909.04(8)
Z	2	4	4
D_{calcd} (Mg/m^3)	1.511	1.936	2.112
μ (mm^{-1})	1.225	1.105	2.450
$F(000)$	492	1048	1176
Goodness of fit on F^2	1.052	1.064	1.003
θ (°)	3.4–626.06	3.71–26.05	3.44–26.06
Reflections collected	7478	5922	14509
Unique reflections	4099	1817	3759
Absorption correction	Analytical	Analytical	Analytical
Solution method	Direct	Direct	Direct
Independent reflections (R_{int})	0.0216	0.0314	0.0743
R_1, wR_2 [$I>2\sigma(I)$]	0.0260, 0.0646	0.0259, 0.0609	0.0364, 0.0798
R_1, wR_2 [all data]	0.0327, 0.0662	0.0286, 0.0622	0.0529, 0.0855
Flack parameter	–	–	0.00(15)
Largest residuals (eÅ^3)	0.345/−0.273	0.594/−0.462	1.197/−0.863

M.p.: 208 °C (dec), Anal. Calcd for $C_{15}H_{16}Cl_4N_4Pd_2$ (**3**) (%): C, 29.68; H, 2.66; N, 9.23. Found (%): C, 29.87; H, 2.59, N, 8.97. IR (KBr, cm^{-1}): 3038, 3021 ($CH_{aromatics}$); 2940 (CH_2); 2850 (CH_2–N); 1632 (C=N); 1609 (C=N, C=C).

3. Results and discussion

Complex **1**·3H_2O was obtained from the reaction of **L** with $NiCl_2 \cdot 6H_2O$ in an equimolar ratio; it was obtained as a green solid soluble in methanol, acetonitrile, and DMSO. Use of hot acetonitrile yielded the diaqua complex **1** instead of the dichloro complex *trans*-[Ni^{II}(**L**)Cl_2]·2H_2O, yielded from the same starting materials (**L** and $NiCl_2 \cdot 6H_2O$) but using ethanol as solvent at room temperature [35]. Complexes **2** and **3** were synthesized from reaction of **L** with [$Pd^{II}Cl_2(CH_3CN)_2$] in equimolar ratio for **2** and a 1:2 ratio for **3** (see scheme 1); both complexes were obtained as yellow solids, moderately soluble in acetonitrile and DMSO. Complexes **1–3** were obtained as stable solids and they can be stored for several months at room temperature.

3.1. *Infrared spectroscopy*

The spectrum of **L** had ν(C=N) at 1649 and 1587 cm^{-1} for imine and pyridine, respectively. In **1–3**, ν(C=N) of imine are shifted to lower energies (1640, 1639, and 1632 cm^{-1})

Table 3. Selected bond lengths [Å] and angles [°] for **1**–**3**.

	1·3H_2O M = Ni	**2** M = Pd	**3** M = Pd
M–N(1)	2.1154(14)	2.059(2)	2.035(6)
M–N(2)	2.0453(15)	1.991(2)	2.014(5)
M–N(3)	2.0508(14)		2.028(5)
M–N(4)	2.1096(15)		2.030(5)
M–Cl(1)	–	–	2.2936(18)
M–Cl(2)	–	–	2.2942(17)
M–Cl(3)	–	–	2.2897(17)
M–Cl(4)	–	–	2.2798(18)
M–(O1)	2.0639(14)	–	–
M–(O2)	2.1150(13)	–	–
C(6)–N(2)	1.261(2)	1.266(3)	1.283(8)
C(10)–N(3)	1.263(2)		1.266(8)
N(1)–M–N(2)	79.59(6)	80.10(9)	80.4 (2)
N(2)–M–N(3)	93.00(6)	–	–
N(2)-Pd(1)-N(2A)		95.00(13)	
N(3)–M–N(4)	79.61(6)		80.5(2)
N(2A)-Pd(1)-N(1A)		80.10(9)	
N(1)–M–N(3)	171.67(6)	–	–
N(2)–M–N(4)	171.98(6)	–	–
N(2A)–Pd(1)–N(1)	–	173.56(8)	–
N(1)–M–N(4)	107.99(6)	–	–
N(1A)-Pd(1)-N(1)		105.09(11)	
N(1)–M–Cl(1)	–	–	175.13(16)
N(2)–M–Cl(2)	–	–	172.01(15)
N(3)–M–Cl(3)	–	–	176.08(16)
N(4)–M–Cl(4)	–	–	172.04(16)
Cl(1)–M–Cl(2)	–	–	90.53(7)
Cl(3)–M–Cl(4)	–	–	95.57(16)
O1–M–O2	177.79(6)	–	–

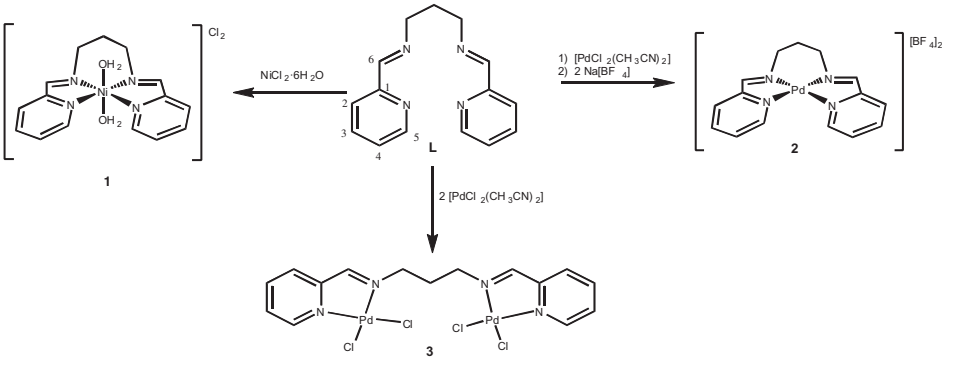

Scheme 1. Synthesis of **1**–**3**.

with respect to **L**. The shift to lower energies has been explained by the decrease of *s* orbital character of nitrogen lone pair in the C=N bond after coordination, increasing the C=N bond lengths [36, 37]. The magnitude of these shifts suggests that the Lewis acidity of Pd^{II} in **2** and **3** is less than that in the Ni^{II} center in **1**.

3.2. *^{1}H and ^{13}C{^{1}H} NMR*

^{1}H and ^{13}C{^{1}H} NMR spectra of **L** and diamagnetic **2** and **3** were obtained at room temperature in DMSO-d_6. The assignment of the NMR signals is given in table 1.

In the ^{1}H NMR spectra of **2** and **3** the pyridine protons were observed at high frequencies compared to those observed in free **L**, exhibiting an ABCD pattern (see Supplementary material, figure 1S). The differences in chemical shifts ($\Delta\delta$) of H3 in **2** and **3** compared to that observed in **L** were 0.69 and 0.53 ppm, respectively. The $\Delta\delta$ measured for H4 were 0.59 ppm (for **2**) and 0.45 ppm (for **3**) and for H6 were 0.60 and 0.51 ppm (for **2** and **3**, respectively). Similar resonance shifts have been reported for other Pd^{II} complexes and they have been attributed to deshielding of coordination [11]. Pyridine and imine protons in **2** were more unshielded than those observed in **3**, attributed to higher number of chelate rings in **2** (two five-membered and one six-membered chelate rings) than **3** (two five-membered chelate rings). The stereochemistry of the C=N_{imine} bond in free **L** can be established by comparison with ^{1}H NMR data of **2** and **3**. Based on the two signals for methylene protons –$CH_2C\mathbf{H}_2N$ and –$C\mathbf{H}_2CH_2N$, in **L** as well as **2** and **3**, the corresponding chemical shifts are quite similar. Thus, if an *E*, *E* stereochemistry is required to chelate Pd^{II}, a similar stereochemistry is expected for free **L** in solution. This proposal is also supported by chemical shifts reported for methylene protons in analogous Pd^{II} complexes derived from imine ligands [24].

In ^{13}C{^{1}H} NMR spectra of **2** and **3** aromatic carbons were also observed at high frequencies compared to **L** (see Supplementary material, figure 2S). Larger $\Delta\delta$ was observed for C6 (11.2 and 9.1 ppm for **2** and **3**, respectively), attributed to coordination [11].

3.3. *X-ray crystallography*

Crystallographic data for **1–3** are summarized in table 2 and selected bond distances and angles are given in table 3. Complex **1** crystallized with three waters. Complex **2** belongs to the C_2 point group; in the unit cell, the –$CH_2CH_2CH_2$– chain exhibits positional disorder, and the palladium and methylenic central carbon lie on a special position.

Crystalline structures in solid state for **1–3** were determined by single-crystal X-ray diffraction analyses. In **1** and **2**, **L** showed tetradentate coordination forming two five-membered chelate rings and one six-membered chelate ring, where pyridine and imine nitrogens are coordinated. In **3**, **L** bridges two palladiums; coordination of pyridylimine moieties exhibited bidentate coordination.

3.3.1. Molecular and crystal structure of 1·3H_2O. In the molecular structure of **1**·3H_2O (figure 1), a nickel complex cation is stabilized by two chlorides. In [$Ni^{II}(N_{pyridine})_2(N_{imine})_2(O_{water})_2$] the local geometry around six-coordinate Ni^{II} is distorted octahedral, with two molecules of water coordinated *trans* [O(1)–Ni(1)–O(2) angle: 177.79 (6)°]. The Ni–$N_{pyridine}$ bond distances [2.1154(14) and 2.1096(15) Å] are significantly longer than Ni–N_{imine} distances [2.0453(15) and 2.0508(14) Å]. The shortening of the Ni–N_{imine} bond has been attributed to π acceptor ability of imine nitrogen which promotes d(metal)→π(C–N_{imine}) back-bonding [28]; this may be enhanced by the *trans* pyridine nitrogen. The Ni-OH_2 bond lengths are significantly different [2.0639(14) and 2.1150(13) Å], possibly because of the different hydrogen-bond network (*vide infra*); these distances are very similar to those described for analogous Ni^{II} aqua complexes [38]. The different bite

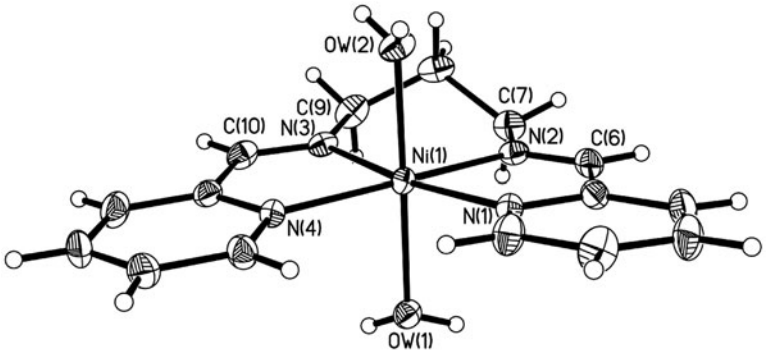

Figure 1. Molecular structure of **1**. The chlorides and three hydration waters are omitted for clarity.

angles reflect the size of the chelate rings formed; for the two five-membered rings the bite angles are 79.59(6) and 79.61(6)°, while for the six-membered chelate ring the bite angle is 93.00(6)°.

The crystal structure of **1**·3H_2O displayed an intricate hydrogen-bond network between coordinated and hydration waters with chlorides (figures 2 and 3 and table 4). In this network, interatomic distances O–O and O–Cl ranged from of 2.648(2) to 2.746(2) Å and

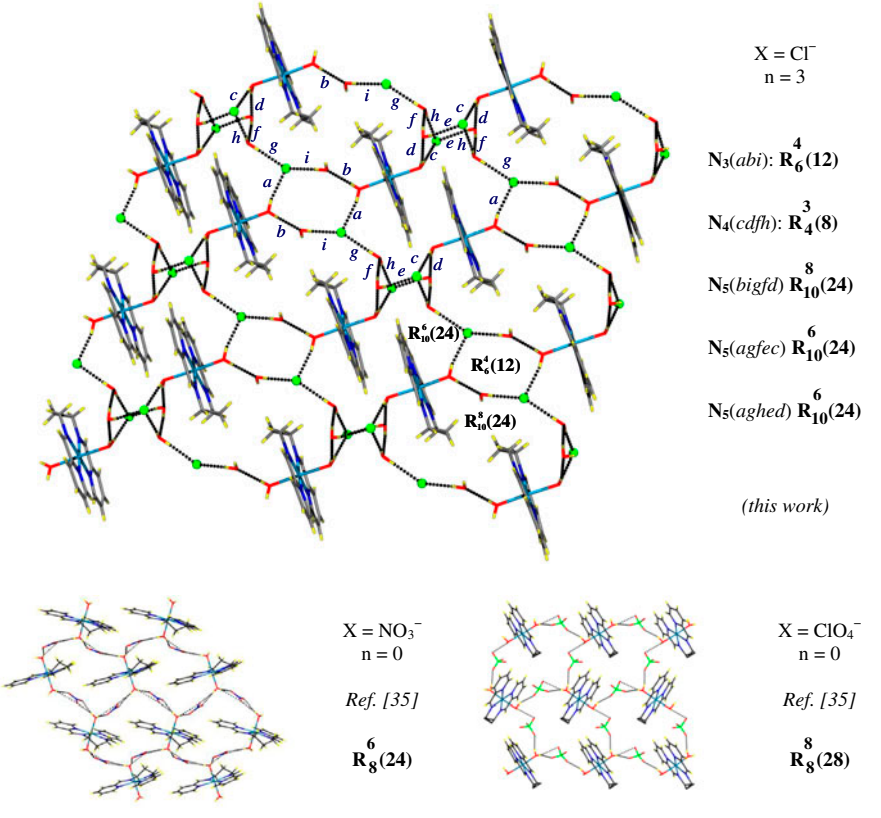

Figure 2. Hydrogen-bond networks in the diaqua complexes $[Ni^{II}(\mathbf{L})(H_2O)_2]X_2 \cdot n(H_2O)$ and graph descriptors.

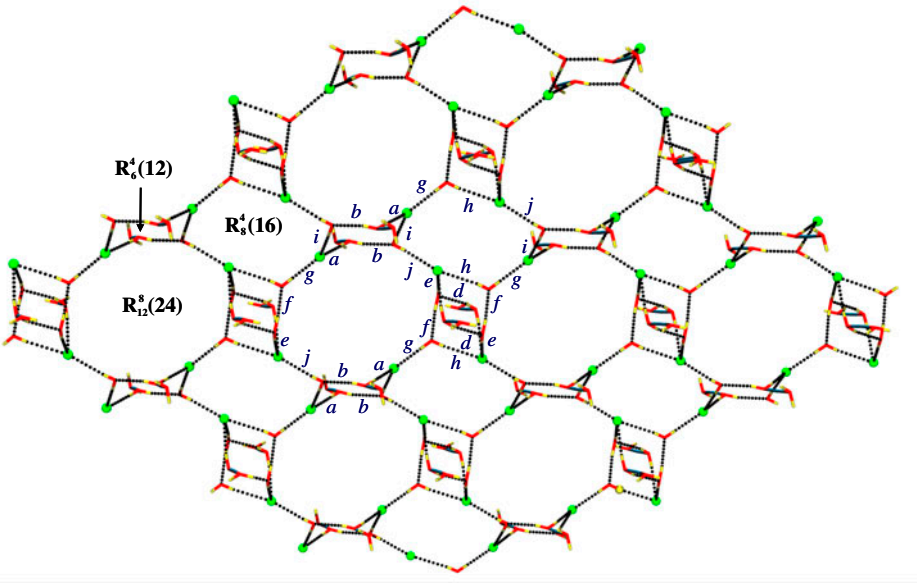

Figure 3. Hydrogen bonding in **1** (for the sake of clarity **L** was removed).

from 3.0826(15) to 3.204(2) Å, respectively; these noncovalent interactions are shorter than the van der Waals radii sum for these atoms [$\sum r_{vdW}$(O, O) = 3.04 Å and $\sum r_{vdW}$(O, Cl) = 3.27 Å] [39]. Figure 2 shows an array of molecules of **1** trihydrate connected by directional hydrogen bonds. $H_2O(1)$ and $H_2O(2)$ are engaged in different centrosymmetric intermolecular arrays. To describe the intermolecular interactions based on hydrogen bonding, we used the graph analysis approach [40]. From the analysis, we recognize 10 distinct hydrogen bonds (*motifs*), alphabetically labeled from *a* to *j* (table 4). The topologically characteristic pattern of the array includes rings of third, fourth, fifth, and even sixth level graph sets. In figure 2 (top) some of these graph set assignments are shown. A very interesting array can be visualized when 2-$C_5H_4NCH{=}N(CH_2)_3N{=}CH$(2-$C_5H_4N$) framework is removed from the crystal structure (figure 3); the water hydration molecules in conjunction with chlorides form a highly puckered hydrogen-bonded layer with several rings, exhibiting different sizes and conformations. These layers are further connected by the H_2O–Ni–H_2O vector, forming a multilayer arrangement.

Lastly, it is interesting to comment about the role of the different anions in the hydrogen bond networks of $[Ni^{II}(\mathbf{L})(H_2O)_2]X_2{\cdot}n(H_2O)$ complexes (X = Cl^-, $n = 3$; X = NO_3^-, $n = 0$; X = ClO_4^-, $n = 0$). We retrieved the data of the crystal structures of nitrate and perchlorate complexes from the Cambridge Structural Database (deposition numbers 693,872 and 693,873, respectively) and redrew the structures by using the Mercury 3.1 software [41]. After analyzing the structures, the two polyatomic anions displayed three N–O and four Cl–O branches that are not crystallographically equivalent and they display three-centered (bifurcated) hydrogen bonds; the chloride in **1** clearly has not this availability. In figure 2 (bottom) the main features of the arrays based on rings for nitrate and perchlorate complexes are shown. The presence of three hydration waters in **1** prompts a more intricate hydrogen bond network.

Table 4. Hydrogen bonds[a] in the crystal structure of $\mathbf{1}\cdot 3H_2O$.

D–H···A interaction	d(D–H)	d(H···A)	d(D···A)	∠ (DHA)	Symmetry code used to generate equivalent atoms	Label
O(1)–H(1A)···Cl(1)	0.80(2)	2.30(2)	3.0826(15)	167(2)	$-x+1, -y, -z+1$	*a*
O(1)–H(1B)···O(5)	0.78(2)	1.88(3)	2.648(2)	168(2)	$-x, -y+1, -z+1$	*b*
O(2)–H(2A)···Cl(2)	0.88(3)	2.32(3)	3.1899(16)	171(2)	$-x+1, -y+1, -z+1$	*c*
O(2)–H(2B)···O(3)	0.78(2)	1.98(2)	2.746(2)	167(2)	$-x+1, -y+1, -z+1$	*d*
O(3)-H(3A)···Cl(2)	0.76(2)	2.40(2)	3.1584(17)	172(2)	$-x+1, -y+1, -z+1$	*e*
O(3)–H(3B)···O4	0.88(3)	1.84(3)	2.711(2)	174(2)	*x*, *y*, *z*	*f*
O(4)–H(4A)···Cl(1)	0.84(3)	2.25(3)	3.085(2)	179(2)	*x*, *y*, *z*	*g*
O(4)–H(4B)···Cl(2)	0.74(3)	2.47(3)	3.204(2)	172(3)	*x*, *y*, *z*	*h*
O(5)–H(5A)···Cl(1)	0.89(3)	2.25(3)	3.1346(19)	177(2)	$-x+1, -y+1, -z+2$	*i*
O(5)-H(5B)···Cl(2)	0.73(3)	2.41(3)	3.1342(19)	175(3)	*x*, *y*, *z*	*j*

[a]O–H hydrogen atoms were refined in difference electron density maps; C–H hydrogen atoms were fixed to the heavy atom.

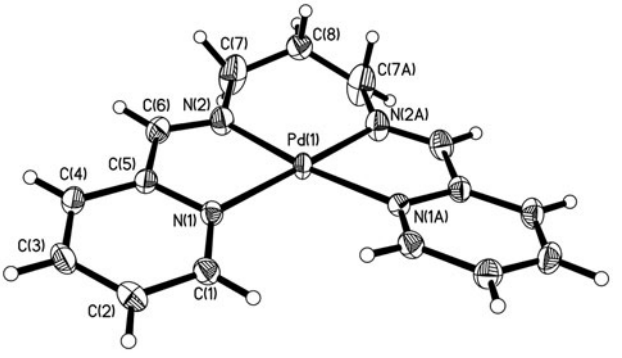

Figure 4. Molecular structure of **2** (the tetrafluoroborates are omitted for clarity).

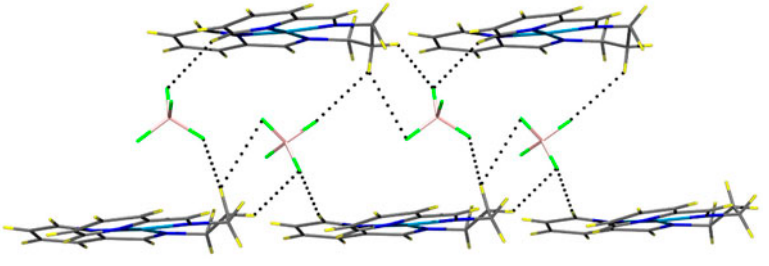

Figure 5. C–H···F interactions in the crystal structure of **2**.

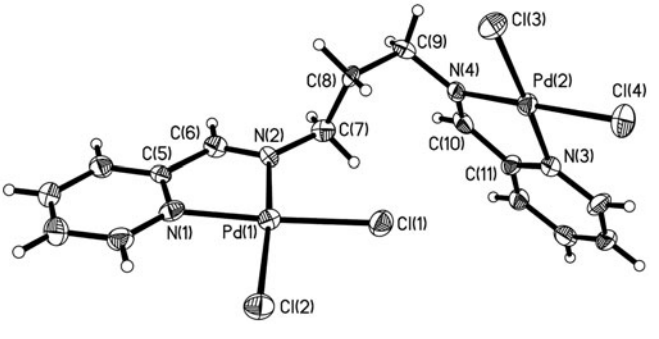

Figure 6. Molecular structure of **3**.

3.3.2. Molecular structure of 2. The molecular structure of **2** is shown in figure 4. In **2**, **L** is tetradentate towards Pd^{II} with the formation of two five-membered and one six-membered chelate rings as in **1**. The geometry of Pd^{II} is distorted square planar; the closest distance with the tetrafluoroborate anions is 3.400 Å. Because of the C_2 symmetry, both five-membered chelate rings displayed the same N(1)–Pd(1)–N(2) bite angles [80.10(9)°], whereas for the six-membered chelate ring the bite angle was 95.00(13)°. The N(2)–Pd–N(2) angle in *trans* position was 173.56(8)°, consistent with the local geometry at the metal. As in **1**, Ni–$N_{pyridine}$ bond distances are significantly longer than Ni–N_{imine} ones. In **2**, the crystal structure is

stabilized by weak C–H···F interactions (figure 5); the distances range from 2.30 to 3.03 Å and the graph set descriptor of the smallest ring is $R_2^2(6)$.

3.3.3. Molecular structure of 3. In figure 6 the molecular structure of **3** is shown. **L** bridges two palladiums and each pyridylimine is bidentate toward each Pd^{II}, forming a dinuclear complex. The local geometry around palladium was distorted square planar. In **3**, the greater conformational freedom, because of no six-membered chelate ring as in complexes **1** and **2**, causes the Pd–$N_{pyridine}$ and Pd–N_{imine} bond distances to be the same. These bond lengths are similar to those observed in a related Pd^{II} complex containing *bis*-(pyridylimine) ligands [10]. The Pd–Cl bond distances ranged from 2.2797(18) to 2.2943(17) Å, very similar to those reported for analogous *cis*-dichloropalladium(II) complexes [1,9,12].

The [N(1)–Pd(1)–N(2) and N(3)–Pd(2)–N(4)] bite angles were 80.4(2) and 80.5(2)°, respectively, while *trans* N(1)–Pd(1)–Cl(1), N(2)–Pd(1)–Cl(1), N(3)–Pd(2)–Cl(3), and N(4)–Pd(2)–Cl(4) angles were 172.01(15)–176.08(16)°; these data are consistent with the distorted square planar geometry around Pd^{II}.

4. Conclusion

New derivatives of Ni^{II} and Pd^{II} containing 1,7-*bis*-(pyridin-2-yl)-2,6-diaza-1,6-heptadiene (**L**) have been synthesized. The molecular structures of **1–3** displayed two coordination modes of **L** toward M^{II} with formation of five- and six-membered chelate rings; these quite different binding modes are consistent with the wide coordination versatility of **L**, where mononuclear Ni^{II} and Pd^{II} (**1** and **2**) and dinuclear Pd^{II} (**3**) complexes were obtained. In the solid state, the presence of hydrogen-donors and acceptors enhance the formation of supramolecular associations. The trihydrate diaqua nickel complex (**1**·$3H_2O$), where the presence of hydration waters in conjunction with the nondirectional nature of chloride creates a wide variety of rings; this pattern is different from those observed in the non-hydrated $[Ni^{II}(\mathbf{L})(H_2O)_2]X_2$ complexes ($X = NO_3^-$, ClO_4^-) previously reported, where the more directional triangular and tetrahedral anions lead to a minor number of motifs and, therefore, to a limited variety of rings.

Supplementary material

CCDC deposition numbers 912918 (**1**·$3H_2O$), 912919 (**2**), and 912920 (**3**) contain the Supplementary Crystallographic Data for this article. These data can be obtained free of charge via http://www.ccdc.cam.ac.uk (or from the Cambridge Structural Data Center, 12 Union Road, Cambridge, CB2 1EZ, UK; Fax: +44 1223 336033).

Acknowledgment

JRPM acknowledges the scholarship from CONACYT. This research was supported by CONACYT (Project 81003).

References

[1] S.J. Scales, H. Zhang, P.A. Chapman, C.P. McRory, E.J. Derrah, C.M. Vogels, M.T. Saleh, A. Decken, S.A. Westcott. *Polyhedron*, **23**, 2169 (2004).

[2] M.L. Conrad, J.E. Enman, S.J. Scales, H. Zhang, C.M. Vogels, M.T. Saleh, A. Decken, S.A. Westcott. *Inorg. Chim. Acta*, **358**, 63 (2005).
[3] M.A. Ali, A.H. Mirza, R.J. Butcher, K.A. Crouse. *Transition Met. Chem.*, **31**, 79 (2006).
[4] U. McDonnell, J.M.C.A. Kerchoffs, R.P.M. Castineiras, M.R. Hicks, A.C.G. Hotze, M.J. Hannon, A. Rodger. *Dalton Trans*., 667 (2008).
[5] B. Samanta, J. Chakraborty, C.R. Choudhury, S.K. Dey, D.K. Dey, S.R. Batten, P. Jensen, G.P.A. Yap, S. Mitra. *Struct. Chem.*, **18**, 33 (2007).
[6] U. McDonnell, M.R. Hicks, M.J. Hannon, A. Rodger. *J. Inorg. Biochem.*, **102**, 2052 (2008).
[7] M. Shakir, M. Azam, S. Parveen, A.U. Khan, F. Firdaus. *Spectrochim. Acta, Part A*, **71**, 1851 (2009).
[8] A. Pal, B. Biswas, S.K. Mondal, C.-H. Lin, R. Ghosh. *Polyhedron*, **31**, 671 (2012).
[9] J. Yorke, C. Dent, A. Decken, A. Xia. *Inorg. Chem. Commun.*, **13**, 54 (2010).
[10] M. Kettunen, C. Vedder, H.-H. Brintzinger, I. Mutikainen, M. Leskelä, T. Repo. *Eur. J. Inorg. Chem.*, **1081**, (2005).
[11] J.M. Sibanyoni, G.B. Bagihalli, S.F. Mapolie. *J. Organomet. Chem.*, **700**, 93 (2012).
[12] S. Abraham, C.-S. Ha, I. Kim. *Macromol. Rapid Commun.*, **27**, 1386 (2006).
[13] D. Tzimopoulos, S. Brenna, A. Czapik, M. Gdaniec, A. Ardizzoia, P.D. Akrivos. *Inorg. Chim. Acta*, **383**, 105 (2012).
[14] T.K. Karmakar, G. Aromí, B.K. Ghosh, A. Usman, H.-K. Fun, T. Mallah, U. Behrens, X. Solans, S.K. Chandra. *J. Mater. Chem.*, **16**, 278 (2006).
[15] M. Habib, T.K. Karmakar, G. Aromí, J. Ribas-Ariño, H.-K. Fun, S. Chantrapromma, S.K. Chandra. *Inorg. Chem.*, **47**, 4109 (2008).
[16] T.K. Karmakar, B.K. Ghosh, A. Usman, H.-K. Fun, E. Riviére, T. Mallah, G. Aromí, S.K. Chandra. *Inorg. Chem.*, **44**, 2391 (2005).
[17] I.I. Ebralidze, G. Leitus, L.J.W. Shimon, Y. Wang, S. Shaik, R. Neumann. *Inorg. Chim. Acta*, **362**, 4713 (2009).
[18] S. Das, K. Bhar, S. Chattopadhyay, P. Mitra, V.J. Smith, L.J. Barbour, B.K. Ghosh. *Polyhedron*, **38**, 26 (2012).
[19] Sk. H. Rahaman, R. Ghosh, T.-H. Lu, B.K. Ghosh. *Polyhedron*, **24**, 1525 (2005).
[20] Sk. H. Rahaman, H. Chowdhury, D. Bose, R. Ghosh, C.-H. Hung, B.K. Ghosh. *Polyhedron*, **24**, 1755 (2005).
[21] S. Oshima, N. Hirayama, K. Kubono, H. Kokusen, T. Honjo. *Anal. Chim. Acta*, **441**, 157 (2001).
[22] M. Pascu, G.J. Clarkson, B.M. Kariuki, M.J. Hannon. *Dalton Trans*., 2635 (2006).
[23] J. Fielden, D.-L. Long, C. Evans, L. Cronin. *Eur. J. Inorg. Chem.*, 3930 (2006).
[24] S. Gourbatsis, S.P. Perlepes, N. Hadjiliadis, G. Kalkanis. *Transition Met. Chem.*, **15**, 300 (1990).
[25] S. Gourbatsis, N. Hadjiliadis, S.P. Perlepes, A. Garoufis, I.S. Butler. *Transition Met. Chem.*, **23**, 599 (1998).
[26] N. Mondal, S. Mitra, G. Rosair. *Polyhedron*, **20**, 2473 (2001).
[27] A. Mukherjee, M. Nethaji, A.R. Chakravarty. *Polyhedron*, **23**, 3081 (2004).
[28] S. Banerjee, J. Gangopadhyay, C.-Z. Lu, J.-T. Chen, A. Ghosh. *Eur. J. Inorg. Chem.*, 2533 (2004).
[29] I.-C. Hwanga, K. Ha. *Acta Cryst.*, **E65**, m64 (2009).
[30] S.I.M. Paris, Ü.A. Laskay, S. Liang, O. Pavlyuk, S. Tschirschwitz, P. Lönnecke, M.C. McMills, G.P. Jackson, J.L. Petersen, E. Hey-Hawkins, M.P. Jensen. *Inorg. Chim. Acta*, **363**, 3390 (2010).
[31] S. Pal, S. Pal. *Polyhedron*, **22**, 867 (2003).
[32] M.G.B. Drew, M.R. StJ, M.J. Foreman, K.K. Hudson. *Inorg. Chim. Acta*, **357**, 4102 (2004).
[33] Oxford Diffraction. *CrysAlis software system* (*Version 1.171.33.31*), Oxford Diffraction Ltd., Abingdon (2009).
[34] Bruker Analytical X-ray Systems. *SMART: Bruker Molecular Analysis Research Tool V. 5.057 c* (1997–98). Bruker Analytical X-ray Systems. *SAINT + NT* (*Version 6.01*) (1999). Bruker Analytical X ray Systems. *SHELXTL-NT* (*Version 5.10*), Bruker AXS Inc., Madison, USA (1999).
[35] R.-L. Zhang, J.-S. Zhao, P. Yang, Q.-Z. Shi. *J. Chem. Crystallogr.*, **40**, 357 (2010).
[36] J.J. Lopez-Carriga, G.T. Babcock, J.F. Harrison. *J. Am. Chem. Soc.*, **108**, 7241 (1986).
[37] W.A. Seth-Paul, B. Van der Veken, M.A. Hermat. *Spectrosc. Int. J.*, **1**, 120 (1982).
[38] N. Andrade-López, T.A. Hanna, J.G. Alvarado-Rodríguez, A. Luqueño-Reyes, B.A. Martínez-Ortega, D. Mendoza-Espinosa. *Polyhedron*, **29**, 2304 (2010).
[39] W.W. Porterfield. *Inorganic Chemistry: A Unified Approach*, 2nd Edn, p. 214, Academic Press, San Diego, CA (1993).
[40] J. Bernstein, R.E. Davis, L. Shimoni, N.-L. Chang. *Angew. Chem. Int. Ed. Engl.*, **34**, 1555 (1995).
[41] Mercury CSD 2.0 – New Features for the Visualization and Investigation of Crystal Structures, C.F. Macrae, I.J. Bruno, J.A. Chisholm, P.R. Edgington, P. McCabe, E. Pidcock, L. Rodriguez-Monge, R. Taylor, J. van de Streek, P.A. Wood. *J. Appl. Cryst*., **41**, 466 (2008).